JCSE The Journal of Corrosion Science and Engineering
ISSN 1466-8858 Volume 16, Preprint 62 submitted 30 September 2013

Effect of friction stir processing on the corrosion behavior of AZ31 magnesium alloys

Ebrahim Eskandari[*1], *Ali Davoodi*[1], *Seyed Mostafa Mousavizadeh Nooghabi*[1]
[1] *Hakim Sabzevari University, Sabzevar/Iran*
[*]ebrahim_eskandari@yahoo.com

Abstract

The effect of processing parameters (rotation speed and travel speed) on the microstructure and corrosion behavior of AZ31 magnesium alloys was investigated. It was found that processing parameters plays a major role in controlling the grain size and corrosion behavior. changing in the rotation rate and travelling speed lead to more grain refinement in nugget zone of FSP samples. The results from corrosion tests demonstrate that all FSP samples had a noble corrosion potential compared to the base alloys. Also with reducing in grain size, passivation zone in polarization curves become longer and polarization resistance from EIS measurement was increase. The results from surface volta potential by means of scanning Kelvin probe force microscopy (SKPFM) and optical micrograph of corrosion morphology showed that present of the intermetalic phases with higher potential relative to the matrix might represent initiation sites for localized corrosion in magnesium alloys.

Keywords: Firiction stir processing, magnesium alloy, corrosion, impedance spectroscopy, AFM

Introduction:

Owing to their high strength-to-weight ratio, good damping capacity and recyclability, magnesium alloys are attractive engineering materials and have a high potential for use as lightweight structural materials in such automotive and aerospace applications. Some of the disadvantages of magnesium is that it has a low creep resistance, low formability, low ductility and poor corrosion resistance[1, 2]. In order to improve its metallurgical properties, methods such as heat treatment, rapid solidification, alloying, grain refinement, severe deformation, etc can be applied[3-6]. Since the use of these techniques can lead to change in the microstructure, it can alter the corrosion behavior of the material. Thus the investigation of corrosion behavior after any operation could result in changes in the microstructure so it is essential to understand the final characterization of the materials. Ambat et .al[7] undertook an investigation to understand the effects of different

ISSN 1466-8858 Volume 16, Preprint 62 submitted 30 September 2013

microstructures of AZ91 magnesium alloys by preparing the die-casting and ingot casting routes on corrosion behavior and found that die-cast materials with smaller grain size and finer β phase offered marginally lower corrosion rate compared to the ingot casting. Other research has been reported to improve the mechanical properties of magnesium alloys with ECAP application, but the corrosion resistance will be significantly reduced[8].

Friction stir processing (FSP) is a relatively new processing technology, it was developed for microstructure modification by localizing grain size refinements and homogenization of precipitate particles, based on principles of friction stir welding[9]. Dhanapal et.al[10] investigated the effects of chloride ion concentration, immersion time and PH on corrosion rate of friction stir welded AZ61. Also Chang Zeng et.al[11] reported the influence of microstructural variations on the corrosion behaviour of friction stir welded magnesium alloy AM50. However, there isn't much literature regarding to the relationship between FSP parameters and corrosion behavior of AZ31 alloy. Therefore, the aim of this investigation is to see how corrosion behaviour can be related to microstructural changes controlled by the welding parameters in AZ31 magnesium alloys.

Experimental:

- **Materials and process**

In this research commercial, wrought plate (0.85 cm thick) of magnesium alloy AZ31B (nominally 3% Al, 1% Zn and 0.5% Mn; balance Mg in weight percent) was processed. Friction stir processing was carried out using a milling machine and non-consumable tools made of high carbon steel. The FSP tool consisted of a 15.5mm diameter shoulder coupled to a 4.9mm diameter pin. The pin stick-out length was 2.5mm with the tool tilted 3◦ away from the direction of the welding travel. Varied processing parameters such as tool rotation speed and travel speed was used in this investigation as indicated in table 1.

Microstructural examination was carried out on cross sections perpendicular to the processing direction. The samples were then manually grounded and polished. A standard reagent made of 4.2g picric acid, 10ml acetic acid, 10ml distilled water and 70ml ethanol (95% concentration) was used to reveal the microstructure of the samples.

In order to observe the microstructure and corrosion optical microscopes were used. The grain size of the samples was measured using the line intercept method.

ISSN 1466-8858 Volume 16, Preprint 62 submitted 30 September 2013

- **Polarization tests**

Corrosion test samples taken from the top surface of the FSPs were encased in epoxy resin. Then specimens were polished using 1500 grit paper to achieve a mirror finish prior to electrochemical testing. Polarization tests were carried out using a Ivium model B08099 potentiostat. The test was conducted in a aqueous solution of common 0.6M NaCl(PH=8.4) and in solution of NaOH 0.01M(PH=11). A typical three electrode cell was used with an Ag/AgCl reference, Pt counter and the specimen was a working electrode. Potentiodynamic polarization curves were measured after 900 second immersions of the sample in the solution to stabilize the initial conditions. The cathodic polarization scan was started from -100 mV relative to the open circuit potential (OCP) and then it was polarized in an anodic direction at a scan rate of 0.5 mV/s.

- **Electrochemical impedance spectroscopy**

The samples were prepared as potentiodynamic polarization tests and then placed in a solution of 3.5% NaCl to the impedance test. It has been reported that results of impedance tests of magnesium alloy consists of an inductive loop which may arise from the partial protection of the surface oxide film[8, 12, 13]. Therefore to eliminate and simplify the loop circuit, 20 mV of cathodic potential is applied to the work piece. The amplitude of the perturbative signal is 10 mV and the measuring frequency range is 0.1-105 Hz.

- **Scanning Kelvin probe force microscopy**

The scanning Kelvin probe force microscopy (SKPFM) is a development of the AFM. The SKPFM technique measures the surface distribution of the Volta potential in a nondestructive manner[14, 15]. Prior to the SKPFM measurements, the samples were polished to a 0.3 μm Al2O3 finish and cleansed in a ultrasonic bath using ethanol. Topography and Volta potential images were measured using a commercial Solver Next AFM, equipped with NT-MDT. All mappings were performed in air at room temperature and relative humidity between 20-30% with commercially available metal-coated cantilevers from NT-MDT. The lift scan height employed was about 50 nm. Topography and Volta potential were sampled with a pixel resolution of 256×256 and with a scan frequency rate of 0.6 Hz.

The selection of the surface area for SKPFM measurements were performed by observing the specimen surface under the optical microscope associated with the scanning Kelvin

ISSN 1466-8858 Volume 16, Preprint 62 submitted 30 September 2013

probe. After recording the surface potential maps, the WSxM software was used to analyze the maps and to reproduce the individual surface potential readings.

Results and discussion:

- **Microstructural obsarvation**

Generally based on microstructural characterization of grains and precipitates, there are three obvious zones: stirred (nugget) zone, thermo-mechanically affected zone (TMAZ), and heat-affected zone (HAZ), they have been identified from crosse sectional of FSP samples. In this study microstructure characterization focused on the nugget zone. Figure 1 shows the microstructure base and FSP samples. The as-received material has a fully recrystalization microstructure with an average grain size of about 25µm (Fig.1(a)). Also, some secondary phases with irregular geometric shapes are observed. Previous studies indicate that these phases were intermetallic particles combined with Fe-Mn-Al[16]. According to the Mg-Al phase diagram, Mg17Al12 intermetalic compounds in AZ31 should be in microstructure but due to their very low amount it is not observed in the microstructure by optical microscope. Microstructure of FSP samples in the stir zones were included, also fully recrystalizationed grain and more homogenous grain structures. The evolution of recrystallized grain structures in the stir zone is due to the severe plastic deformation and frictional heat introduced by the rotating tool pin and its shoulder in the stir zone during FSP[17]. Figure 1 (b-e) shows the microstructures of the NZs under different processing parameters. Grain size of nugget zone for samples 1-4 is 5, 9.8, 13.8 and 18.7 µm respectively and No intermetalic phase obvious in microstructure of FSP samples.

Darras et al. investigated the temperature histories for friction stir processed samples at different rotational and translational speeds and observed the peak temperature increases as the rotational speed increases and the translational speed decreases[18].They also found that, heating and cooling rates as well as the time the materials is exposed to a high temperature are very important to control grain growth [18]. Thus increasing rotation speed and decreasing translational speed caused grater heat input and promotes grain growth[19, 20].

Wang et.al[21] reported that intermetallic compounds tend to disappear due to dissolution at elevated temperature and also the second phase, which is a brittle phase. When applied

stress is higher than the fracture strength of the second phase, fracture takes place and large second phases change into smaller ones gradually. For this reason, after FSP, these phases are not observed in microstructure of SZ zone.

- **The Open-Circuit Potential (OCP)**

The overall corrosion mechanism of magnesium alloys in aqueous environments generally proceeds the electrochemical reaction with water to produce hydrogen gas and magnesium hydroxide according to following equations [14, ASM] :

$Mg \rightarrow Mg^{2+} + 2e$ (anodic reaction) (1)

$2H_2O + 2e \rightarrow H_2 + 2OH^-$ (cathodic reaction) (2)

$Mg^{+2} + 2OH^- \rightarrow Mg(OH)_2$ (product formation) (3)

Fig .2 shows the time variation of Ecorr for all samples during 900 s of immersion in 3.5% NaCl solution. When the samples immersion in the solution, magnesium dissolution takes place immediately and hydrogen evolution is associated with Mg dissolution. As shows in fig .2 at the initial time of immersion, potential decreases rapidly with magnesium dissolution. With the increase of magnesium dissolution and hydrogen evolution, according to equation (1) and (2), The pH increases due to production of OH-,which favors the formation of Mg hydroxide film (equation 3).

Since chlorine is causing destruction of the passive layer, the comprative is between formation and dissolusion of passive layer during the immersion time. In all samples except specimen 1 and 2 corrosion potential decreases with the time until an equilibrium occures between dissolution and precipitation of protective film witch result in potential reaches a constant value.

The fluctuation in OCP value in samples 1 and 2 in the beginning time could be attributed to the dissolution of the passive film and a subsequent exposure of a bare metal surface but with time potential increased and become more stable. This behavior is attributed to passivation of the film possibly because the formation of the corrosion product film could act as an effective barrier to further corrosion[22].

The free corrosion potential in Fig.1 are calculated and listed in Table 2. It is indicated that the Ecorr is ranked as: as-received ＜sample 4＜sample 3＜sample 2＜sample 1.

ISSN 1466-8858 Volume 16, Preprint 62 submitted 30 September 2013

Fig .2 shows the sample with lower grain size and as having a noble corrosion potential compared to the other samples.

- **Polarization curves**

Figure 3a shows the potentiodynamic scan curves of different FSP samples after immersed in 0.6 M NaCl solution for 900 s. The shape of the curves suggests uniform anodic dissolution with a passive like behavior in the anodic branch before showing a break-down. The passive-like behavior can be related to the stability of the passive film, when the sample is exposed to a corrosive environment, Cathodic reaction is the production of (OH)- and hence PH is increased and film is more stable. Based on the anodic and cathodic curves, the corrosion appears to be controlled by the anodic process. There is not a significant difference in cathodic reaction kinetics for all of the samples. However, their anodic reaction kinetics and potential of break-down is various. Table 2 shows the data curves in Figure 3 and icorr calculated form models extrapolation. The test results indicate that the corrosion rate of the as-received is higher than the FSP samples. Also FSP samples showed a more noble corrosion potential, break-down potential and lower corrosion rate than as-received. This suggests that the FSP samples shows more corrosion resistance than as-received alloy.The most of passivation region is related to sample 1 with smaller grain size. With increasing grain size in the FSP sample, the passivation zone become smaller and corrosion potential more active, but no significant changes in corrosion rate between FSP samples. This may be due to the effects of NDE in magnesium alloys, that the corrosion rate of the samples cannot be measured correctly by the polarization method[23].

Fig .3b shows the polarization curves of FSP and as-received samples with grain size of 5 and 25 µm respectively in 0.01 M NaoH(PH=11) .Fig. 2b indicate the flat region passivation in the anodic branch of both samples. According to pourbaix diagram, magnesium in PH above 9 covered with a protective film[23]. The current of passivation in FSP sample and base metal were $6\times10-6$, $3\times10-5$ A cm-2 Respectively, It is apparent (or this attribute to) that the film formed on the FSP sample with finer grain size more stable and protective than as-received sample with larger grain size.

Liao et al[24] investigated corrosion resistance of fine grain AZ31 alloy and they found that the corrosion resistance of AZ31B alloy tends to increase as grain size is reduced, probably due to the enhanced passivity of surface oxide film. Also the dissolution of Mg17Al12 phase in magnesium matrix because of the higher temperatures during FSP, which can increase corrosion resistance. Mathieu et.al.[25] reported that the corrosion rate of the solid solution alloys depends closely on their Al content and Aluminium enhances the corrosion

ISSN 1466-8858 Volume 16, Preprint 62 submitted 30 September 2013

resistance of the a-phase through the formation of an Al enriched superficial layer. This argument may be corrected, for lower corrosion resistance of sample 4 than as-received metal that have close grain size, same passivation width and corrosin potential.

As the grain size of magnesium alloys is reduced, the passivity of surface film seems to be enhanced because the breakdown potential of the passive film is increased.

- EIS measurement

Electrochemical impedance spectroscopy(EIS) is a nondestructive technique with small perturbative signal in order to investigate corrosion behavior. Since magnesium is a very active metal and due to the NDE phenomena in this alloys, Corrosion rate measurements using a polarization technique is combined with error. Therefore, EIS can be a good technique to compare the corrosion behavior of the samples.

Fig. 4 shows the electrochemical AC impedance measurements of AZ31 with various conditions in the 3.5wt.% NaCl solution. The plots of EIS for all sample exhibit one loop capacitance and indicating same corrosion mechanism for all sample. The equivalent circuit model for this plot is include a resistor(Rct) in parallel with the capacitor(Cdl) in series with the solution resistance(Rs). The diameter of a capacitive loop in the Nyquist plane represents the polarization resistance of the test specimens. A greater polarization resistance normally means a larger corrosion resistance. the diameter of a capacitive loop in the Nyquist plane for all FSP samples are much larger than that of as-received alloy, which signifies that the corrosion rate of FSP samples are much lower than as-received alloy. Also with increasing grain size in FSP samples, diameter of loop capacitance become lower. According to Table.3 sample 1 has higher charge transfer resistance value in comparison to other sample, indicating that FSP samples with lower grain size has better corrosion resistance in comparison to as-received and other FSP sample. These results are good agreement with the polarization data in Fig .3.

Argade et. Al reported the mismatch between the surface passive layer and metallic layer underneath is expected to reduce with introduction of large volume fraction of grain boundaries. This leads to better adherence of passive layer and thus it contributes to lower the corrosion rates [26].Liao et.al[24] investigated corrosion behavior of fine-grained AZ31B magnesium alloy and found that film formed on the surface of magnesium alloys consists of a thin inner magnesium oxide (MgO) layer and due to the Pilling Bedworth ratio of MgO to Mg metal is 0.8, the free volume mismatch between MgO and Mg substrate, arising when the MgO forms, causes tensile stress in the MgO layer, thereby increasing its

propensity for cracking. A fine-grained microstructure by producing porosity through vacancy supply via grain boundaries, thus reducing the degree of the MgO layer cracking. So The initial MgO layer formed on the fine-grainedmagnesiumalloy surface provides better surface coverage, and is less prone to cracking or provides a means to inhibit subsequent rupture of the exterior Mg(OH)2 layer.

Gollapudi, [27] show that grain size distribution can assume an important role in the corrosion behaviour of materials. For the same grain size a broader grain size distribution is more corrosion resistant than a narrow grain size distribution in a non-passivating environment. The reverse behaviour is predicted in a passivating environment.As respects FSP lead to more homogenous grain structure, therefore can facilitate the formation of the passive layer.

- **SKPFM measurement**

The corrosion resistance of magnesium alloys has been reported to be influenced by the alloy microstructure, microconstituents, including Fe, Ni, Cu, Si and Co as well as the environment [28, 29]

Figure 5a shows the volt potential map from the AZ31 Magnesium alloy, in the picture there are small zones with high potential compared to the other surface. According to the volta potential line measurement as show in fig 5(b) and (c) the average surface potential values of the micro-constituents, are 70 and 180 mV relative to the adjacent magnesium matrix.

Andreatta et. al. [30] characterized the surface, revealing the potential differences for different intermetallic phases present in the microstructure of AZ80 magnesium alloy, showing that the intermetallic phases exhibited positive surface potentials relative to the magnesium matrix and, in turn, higher cathodic activity compared with the magnesium matrix. In some literature reported the micro-constituents with greater potential as to Al-Mn intermetallics and lower potential as to β-Mg17Al12 phase[31]. Both the micro-constituents, cathodic to the magnesium matrix and indicate a noble behavior[23, 25, 32]. The Al-Mn intermetallics because of more different potential showed the strongest cathodic behavior and have a more destructive effects compare to the other phase.

- **Corrosion morphology**

Fig 6 show Optical micrograph of AZ31specimen surface after immersed in 0.6 M NaCl solution for 2 and 5 min. as indicated that corrosion initiated near the intermetalic phase (fig .5 a) and disperse as filiform corrosion. it is suggested that the cathodic phases are

ISSN 1466-8858 Volume 16, Preprint 62 submitted 30 September 2013

effective sites for the initiation of localized corrosion in AZ31 magnesium alloys. Therefore the corrosion attack of the magnesium matrix was influenced by the surface potential of the intermetallics phases and corrosion initiation from the adjacent this phases.

Conclusions:

In this work the effect of FSP on the microstructure and the corrosion properties of the AZ31 alloy have been studied. The processing parameter has been changed. Microstructural studies exhibits that the cross sectional of FSP region included different area. The FSP microstructure included equiaxed grain recrystallization which the grain size was depended on the processing parameters. In this investigate the grain size of FSP region change with modifying FSP parameters. The results show that increasing in rational rate and decreasing in traveling speed perform that the cooling rate was decrease and indeed growing in grain recrystallization. Corrosion studied exhibit that FSP cusses in increasing corrosion resistance. The corrosion resistance for samples with different FSP parameters is not the same. For the sample with 630 rpm rotational rate and 630 mm/min traveling speed, corrosion resistance twice greater than base metal. Result shows that increasing in corrosion resistance depends on homogenization and grain refinement in the FSP samples. The grain refinement cusses better operation for passive film and increasing in corrosion resistance. Also results from SKPFM measurement shows that intermetalic phases in the microstructure with higher absolute potential in the magnesium surface alloys act as a cathode and can be place for corrosion initiation.

JCSE The Journal of Corrosion Science and Engineering
ISSN 1466-8858 Volume 16, Preprint 62 submitted 30 September 2013

Table 1: FSP parameters

Sample no.	Rotation rate rpm	Traverse speed mm/min
1	630	630
2	630	315
3	1000	250
4	1600	200

Table 2: OCP values

samples	As-received	1	2	3	4
OCP values (v)	-1.57	-1.51	-1.53	-1.55	-1.56

Table 3: Electrochemical parameters from polarization curves for different FSP samples.

Sample conditions	Corrosion potential E_{corr} (mV vs.SCE)	Current density i_{corr}(A/cm^2)	Breakdown potential E_b(mV vs.SCE)	(E_{corr} - E_b)
As-received	-1547.7	2.55*10^-5	-1447	100.7
1	-1490.9	1.1*10^-5	-1326	164.9
2	-1509.4	8.9*10^-6	-1360	149.4
3	-1503.4	8.3*10^-6	-1352	151.4
4	-1541.8	4.3*10^-6	-1452	93.2

Table 4: Fitted results of EIS of FSP and as-received sample.

Sample conditions	Solution resistance R_s (ohm cm^2)	charge transfer resistance R_{ct} (ohm cm^2)	n	C
As-received	15	843	0.96	$2.72*10^{-6}$
1	19.5	1690	0.95	$7.33*10^{-7}$
2	18	1420	0.95	$1.35*10^{-6}$
3	22	1120	0.92	$4.68*10^{-7}$
4	19	930	0.96	$1.15*10^{-6}$

JCSE The Journal of Corrosion Science and Engineering
ISSN 1466-8858 Volume 16, Preprint 62 submitted 30 September 2013

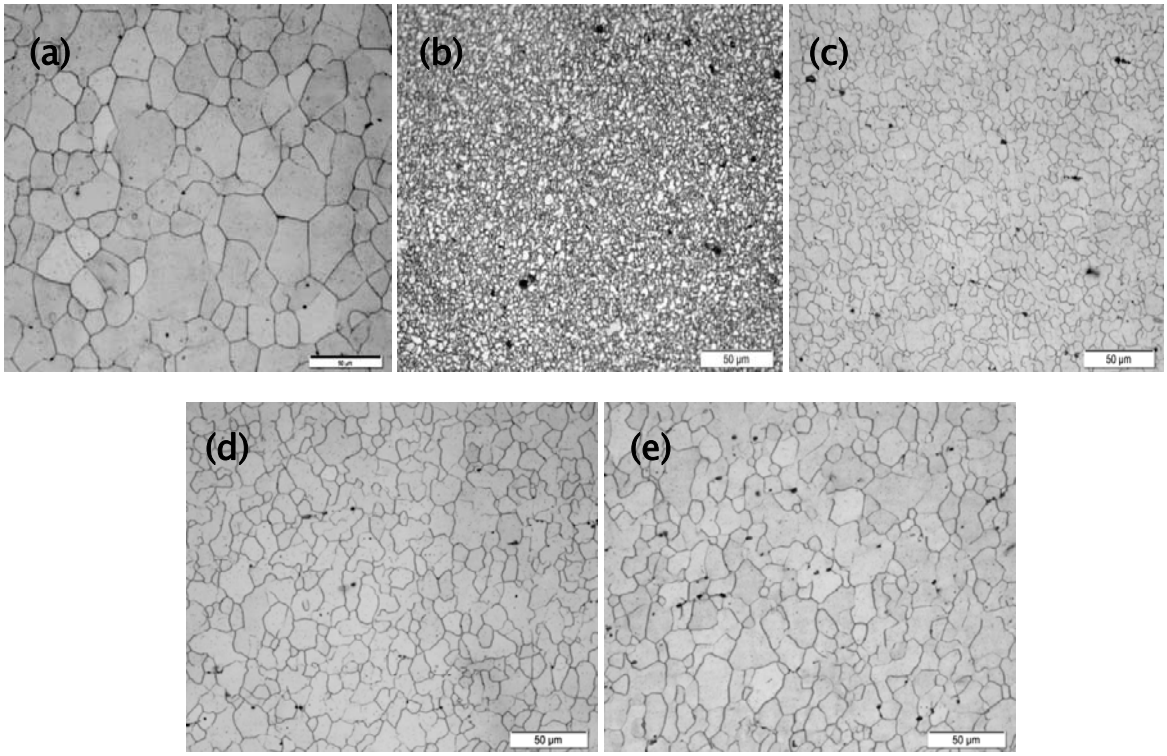

Fig. 1: Microstructure of (a) as-received and FSP sample at (b) 630 rpm, 630 mm/min (c) 630 rpm, 315 mm/min (d) 1000 rpm, 250 mm//min (e) 1600 rpm, 200 mm/min

JCSE The Journal of Corrosion Science and Engineering
ISSN 1466-8858 Volume 16, Preprint 62 submitted 30 September 2013

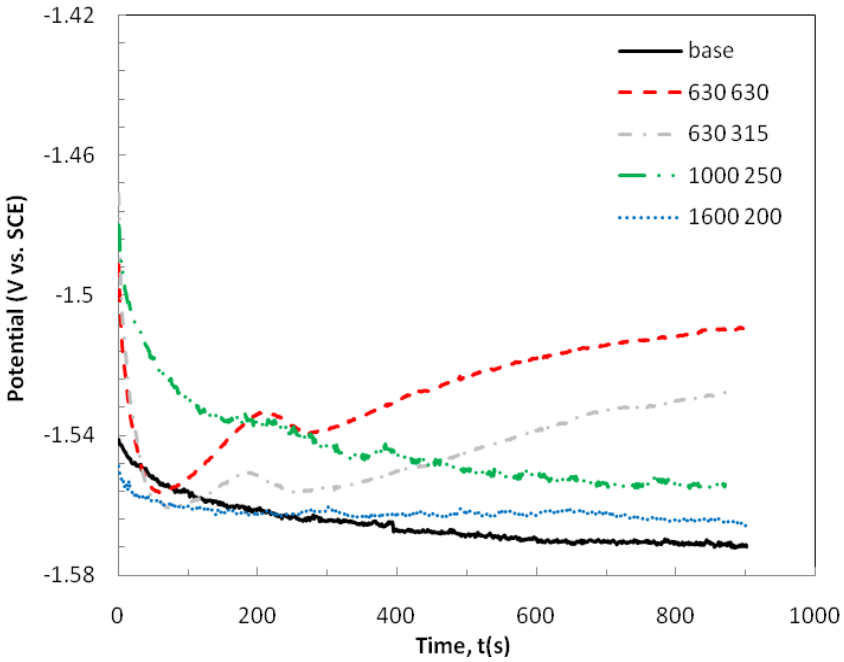

Fig 2: Time variations of open-circuit potentials on different samples in 0.6M NaCl solutions.

JCSE The Journal of Corrosion Science and Engineering
ISSN 1466-8858 Volume 16, Preprint 62 submitted 30 September 2013

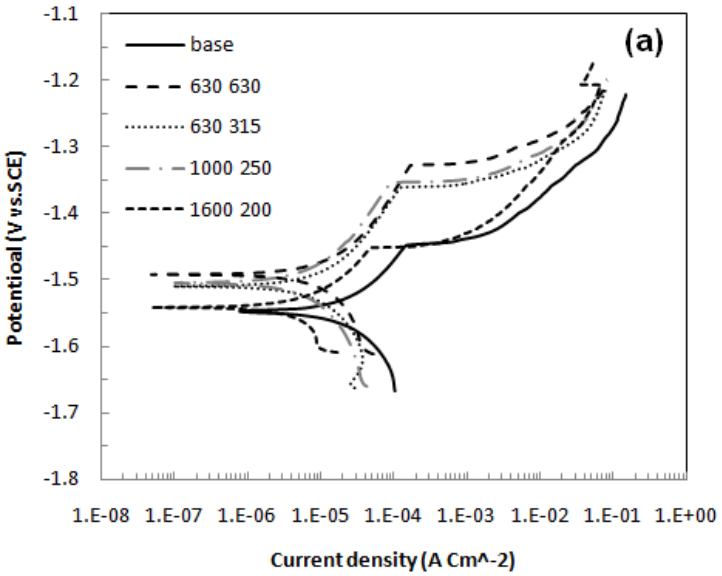

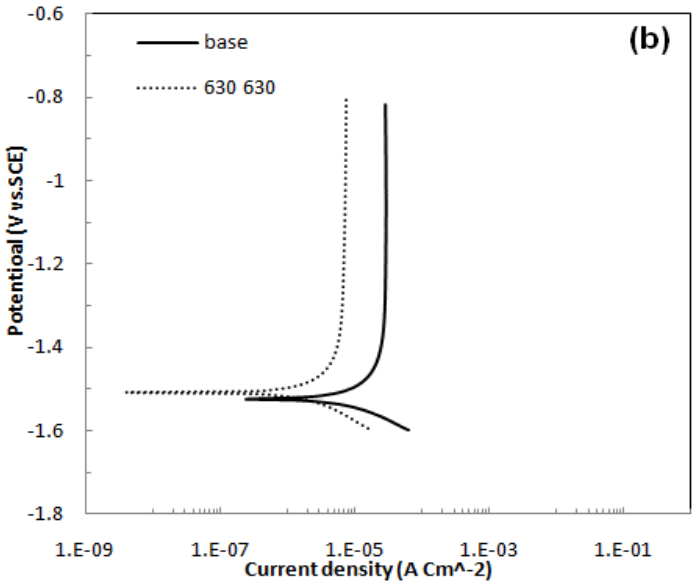

Fig .3 : Potentiodynamic polarization curve of AZ31 Mg alloys immersed in: a) 0.6 M NaCl b) 0.01 M NaoH solution

JCSE The Journal of Corrosion Science and Engineering
ISSN 1466-8858 Volume 16, Preprint 62 submitted 30 September 2013

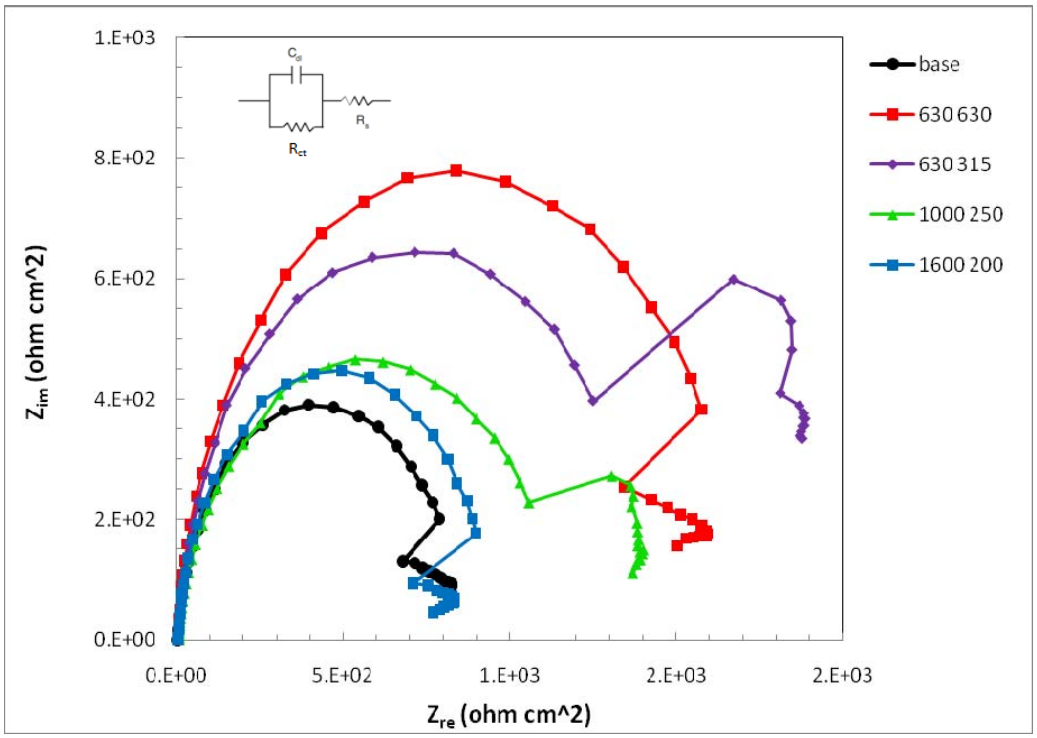

Fig .4: Nyquist plots comparing the corrosion behavior of samples: as-received and four FSP samples

JCSE The Journal of Corrosion Science and Engineering
ISSN 1466-8858 Volume 16, Preprint 62 submitted 30 September 2013

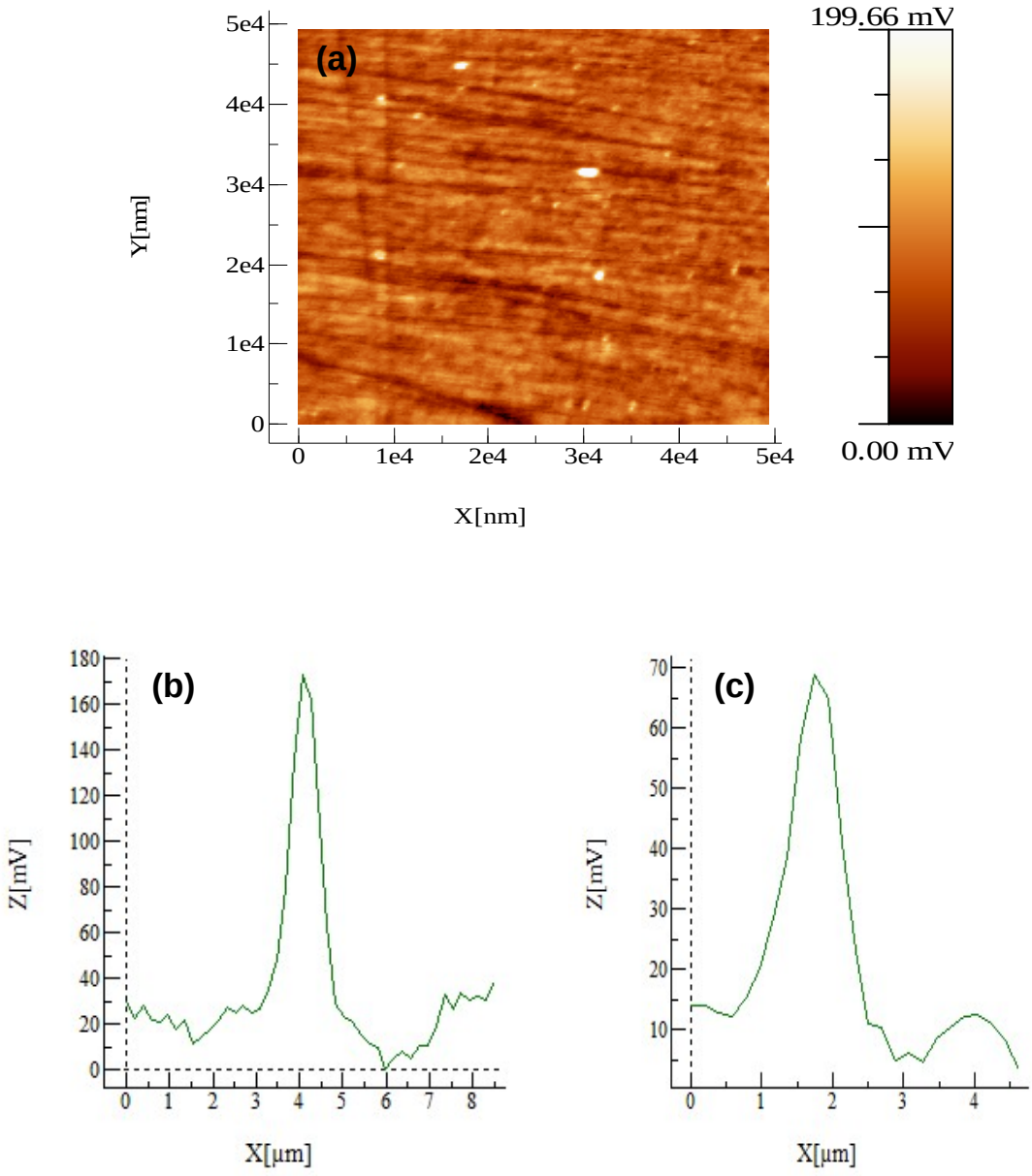

Fig .5: SKPFM study of AZ31 magnesium alloys a) 2D surface potential maps (b) and (c) line profile surface potential

JCSE The Journal of Corrosion Science and Engineering
ISSN 1466-8858 Volume 16, Preprint 62 submitted 30 September 2013

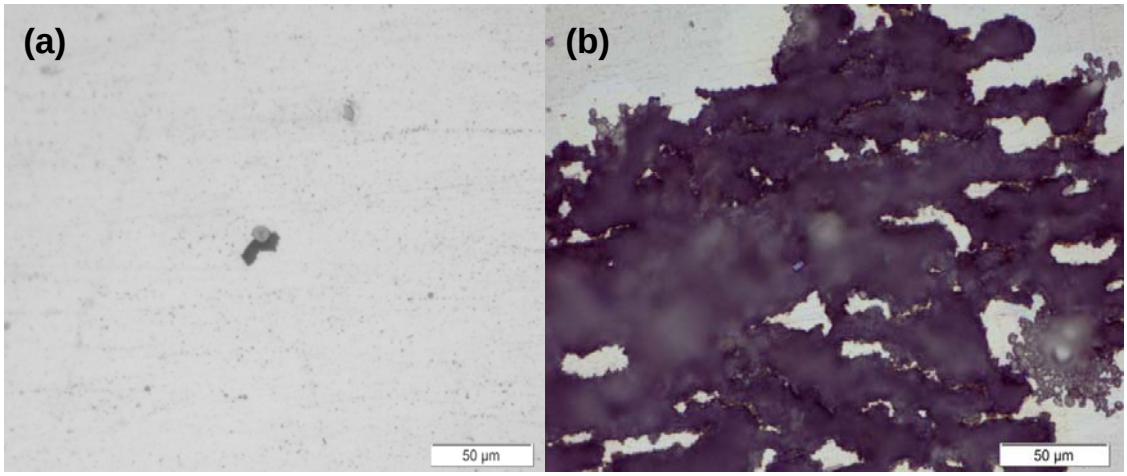

Fig 6: Corrosion morphology of base alloys immersed in 3.5% NaCl after a) 2 min b)5 min.